AAPS PharmSciTech (2024) 25:27
https://doi.org/10.1208/s12249-024-02735-8

RESEARCH ARTICLE

# Development of a PVA/PCL/CS-Based Nanofibrous Membrane for Guided Tissue Regeneration and Controlled Delivery of Doxycycline Hydrochloride in Management of Periodontitis: *In Vivo* Evaluation in Rats

**Shahla Mirzaeei[1,2] · Shadman Pourfarzi[3] · Morteza Saeedi[4] · Shiva Taghe[4] · Ali Nokhodchi[5,6]**

Received: 9 October 2023 / Accepted: 21 December 2023 / Published online: 30 January 2024


## Abstract

Antibiotic administration is an adjacent therapy to guided tissue regeneration (GTR) in the management of periodontitis. This is due to the major role of pathogen biofilm in aggravating periodontal defects. This study aimed to fabricate a GTR membrane for sustained delivery of doxycycline hydrochloride (DOX) while having a space-maintaining function. The membranes were prepared using a polymeric blend of polycaprolactone/polyvinyl alcohol/chitosan by the electrospinning technique. The obtained membranes were characterized in terms of physicochemical and biological properties. Nanofibers showed a mean diameter in the submicron range of < 450 nm while having uniform randomly aligned morphology. The obtained membranes showed high strength and flexibility. A prolonged *in vitro* release profile during 68 h was observed for manufactured formulations. The prepared membranes showed a cell viability of > 70% at different DOX concentrations. The formulations possessed antimicrobial efficacy against common pathogens responsible for periodontitis. *In vivo* evaluation also showed prolonged release of DOX for 14 days. The histopathological evaluation confirmed the biocompatibility of the GTR membrane. In conclusion, the developed nanofibrous DOX-loaded GTR membranes may have beneficial characteristics in favour of both sustained antibiotic delivery and periodontal regeneration by space-maintaining function without causing any irritation and tissue damage.

**Keywords** controlled delivery · doxycycline hydrochloride · guided tissue regeneration · nanofiber · periodontitis

✉ Shahla Mirzaeei
shahlamirzaeei@gmail.com; smirzaeei@kums.ac.ir

✉ Ali Nokhodchi
a.nokhodchi@sussex.ac.uk; AliNokhodchi@lupin.com

1 Nano Drug Delivery Research Centre, Health Technology Institute, Kermanshah University of Medical Sciences, Kermanshah, Iran

2 Pharmaceutical Sciences Research Centre, Health Institute, Kermanshah University of Medical Sciences, Kermanshah, Iran

3 Student Research Committee, School of Pharmacy, Kermanshah University of Medical Sciences, Kermanshah, Iran

4 Pharmaceutical Sciences Research Center, Rahesh Daru Novine, Kermanshah, Iran

5 Lupin Pharmaceutical Research Inc., 4006 NW 124th Ave., Coral Springs, Florida 33065, USA

6 School of Life Sciences, University of Sussex, Brighton BN1 9QJ, UK

## Introduction

Periodontitis is a common disease related to the oral cavity defined as chronic inflammation of tissues surrounding the tooth that may lead to a defect in the gingiva, alveolar bone, alveolar ligament, and eventually tooth loss [1, 2]. As this ailment is highly prevalent worldwide and known as a major cause of tooth loss, the development of novel therapeutic methods and devices for this disease was always the center of interest for health specialists [3, 4]. Periodontitis usually comes across complications such as loss of supporting structures of teeth. The conventional therapeutic methods include surgical and non-surgical procedures, which usually lead to non-specific regeneration of tissues. In fact, the regeneration may take place in a manner that does not match the types of tissue that are lost. Hence, novel treatment methods have been developed [5].

Guided tissue regeneration (GTR) is the most promising therapeutic method for periodontitis management, which is defined as the placement of a biocompatible membrane surrounding an affected tooth to maintain the suitable space for the regeneration of periodontal tissues. GTR membranes genuinely inhibit epithelial cells from growing into the defect and promote the reconstruction of alveolar bone and ligament by creating a supportive wall for tissue regeneration [6, 7]. GTR was first defined by Hurley *et al*. in the 1950s. A membrane barrier was utilized to physically separate soft tissues from the areas of the spine where osteogenesis was active [8]. GTR was first introduced to regenerate periodontal tissue in the 1980s and has since gained acceptance for treating periodontal lesions [9].

It is now well established that pathogens like *Porphyromonas gingivalis* (*P. gingivalis*), *Aggregatibacter actinomycetemcomitans* (*A. actinomycetemcomitans*), *Actinomyces viscosus* (*A. viscosus*), and *Prevotella intermedia* (*P. intermedia*) could be associated with more severe forms of periodontitis [10, 11]. Therefore, antibiotic therapy is considered adjacent to methods like GTR. Local antibiotic therapy with antibiotics such as doxycycline and tetracycline is favoured in light of multiple benefits including lower side effects, more targeted delivery, and higher patient compliance, especially in case of infections that are more focused on a specific site [12, 13]. Mirzaeei *et al*. have recently published a review article on drug-loaded GTR membranes and they concluded that most of the recent studies aimed to develop antibiotics-loaded GTR membranes, due to the confirmed involvement of pathogens in severe forms of periodontitis [14].

According to the information provided earlier, loading antibiotics in GTR membranes would facilitate achieving both space-maintaining and antibiotic delivery functions. Nanofibers are promising uniform drug carriers with suitable thickness, strength, and flexibility which can be used as GTR membranes where these membranes can be fabricated by an efficient method such as electrospinning [15]. Although there are numerous ways to prepare nanofibers, such as phase separation, drawing, and self-assembly, electrospinning has always been one of the most widely used techniques [16]. Electrospinning is a promising method for the preparation of nanofibers as it is convenient, cost-effective, and versatile in the spinning of multiple biocompatible and biodegradable polymers [16, 17]. Guided tissue regeneration (GTR) involves the use of membranes to support tissue regeneration, necessitating specific properties for proper healing. These membranes should be biocompatible to integrate into tissues without causing inflammation. They must also degrade at a rate matching tissue regeneration. Additionally, they should possess appropriate mechanical and physical properties for *in vivo* placement and function as barriers against the growth of epithelial and connective tissues. High resistance to tearing and rupturing during surgery is crucial. Moreover, the membranes should be porous to facilitate cellular adaptation and allow sufficient nutrient permeation. As mentioned before, nanofibers comprised of biocompatible polymers allow the penetration of oxygen and nutrients that are essential for cell growth, but they do not let the cells pass through; hence, they would have suitable structures for GTR. Prepared nanofibrous membranes also have high mechanical properties [18].

Polycaprolactone is a suitable polymer that was employed for manufacturing nanofibrous GTR membranes for the delivery of metronidazole [19]. Another promising biocompatible and biodegradable polymer for the preparation of drug-loaded GTR membranes is polyvinyl alcohol which has been previously used for controlled delivery of tetracycline hydrochloride in the management of periodontists owing to the high potential for obtaining high strength and flexible membranes [20]. Chitosan is one of the most studied biopolymers for tissue engineering. Chitosan is a chitin derivative with a slight antimicrobial effect that can be formulated as GTR membranes as a matrix component and an antiseptic agent [21, 22]. The authors believed that mixing these polymers with a specific ratio provided more efficient GTR membranes with a controlled release manner and antibacterial efficacy. An earlier study examined the drug loading and release characteristics of freeze-cast chitosan scaffolds at various glutaraldehyde percentages [23]. Another study utilized immobilized thiol groups on chitosan and hyaluronic acid polymer backbone to create a thiolated periodontal doxycycline membrane [24].

The current research aimed to create a solution that bridges the gap between efficient drug delivery and optimal periodontal regeneration. A dual-functional nanofibrous GTR membrane engineered to release doxycycline in a controlled manner while providing the essential space-maintaining function holds the promise of transforming periodontal treatment and elevating patient outcomes to new heights. The study's innovative blend of materials, strategic use of electrospinning, and comprehensive evaluations beckon a new era in the management of periodontitis, offering renewed hope for those battling this pervasive oral health ailment. The membranes were prepared using a combination of polymeric blends, including polycaprolactone, polyvinyl alcohol, and chitosan, through the electrospinning technique. The fabricated membranes underwent characterization for mechanical properties and *in vitro* release profiles of the drug. Furthermore, the antibacterial efficacy of the membranes against common periodontal pathogens was investigated. *In vivo* evaluation was conducted using a rat replacement model to assess the drug's release profile in the surrounding tissues and potential irritation and damage in the underlying tissues.

## Materials and Methods

### Materials

Doxycycline (DOX), polyvinyl alcohol (PVA; with a molecular weight of ~ 72,000 g/mol, 98% hydrolyzed), polycaprolactone (PCL; with a molecular weight of 80,000 g/mol), chitosan (CS; with medium molecular weight), trypsin 3-(4,5-dimethylthiazol-2-yl)-2,5-diphenyl-2H-tetrazolium bromide (MTT), and Dulbecco's modified eagle's medium (DMEM) were purchased from Sigma-Aldrich (Germany). Dichloromethane (DCM), N, N dimethylformamide (DMF), acetone (ACT), acetic acid (Assay, 100%), formaldehyde, diethyl ether, sabouraud dextrose broth (SDB), tryptic soy broth (TSB), tryptic soy agar (TSA), fluid thioglycollate medium (FTM), and sodium dihydrogen phosphate dodecahydrate were obtained from Merck (Germany). Fetal bovine serum (FBS) was purchased from Gibco (USA). Penicillin and streptomycin were obtained from Jaber ibn Hayan (Tehran, Iran). Anaerocult® A gas pack was obtained from Merck (Darmstadt, Germany) to provide anaerobic conditions. All materials were purchased in the analytical grade.

### Preparation of DOX-Loaded GTR Membranes

Different drug-to-polymer ratios and solvent mixtures were utilized for the preparation of nanofibers and among them, those that were able to form nanofibers with suitable characteristics were selected for the preparation of GTR membranes. Two different polymeric blends including PVA-PCL and PVA-PCL-CS were utilized to prepare membranes. To prepare the PVA/DOX electrospinning solution, PVA aqueous solution (10% w/v) was prepared under stirring conditions for 12 h, followed by the addition of DOX to the mixture at 20% w/w of PVA. The mixture was stirred until all solid materials were completely dissolved. PVA/CS/DOX solution was also prepared according to the PVA-DOX mixture described above followed by the addition of CS 2% w/v solution in acetic acid (1% v/v) with a mixing ratio of 1:1. PCL (10% w/v) was also completely dissolved in a solvent mixture of DCM: DMF: ACT (4:5:1 v/v) within 3 h.

Both membranes were fabricated by a dual-source, dual-power electrospinning device. In this process, PVA/DOX and PCL solutions were filled in two frontal nozzles for the preparation of the PVA-PCL formulation while for the preparation of PVA-PCL-CS formulation, the nozzles were filled with PVA/CS/DOX and PCL solutions. The solutions were ejected at a rate of 0.2 mL/h toward a rotating collector (200 rpm) wrapped in aluminium foil. A high DC voltage of 20 kV was applied between the injector and collector and the distance between them was kept at 15 cm. The injector swept in a 10-cm range. The whole procedure was performed at 25°C temperature.

### Physicochemical Characterization

#### Scanning Electron Microscopy (SEM)

The morphology and diameter of prepared fibers were examined using a SU3500 SEM device (Hitachi, Japan). To prepare the samples for SEM image, first, they were gold-coated followed by placing in a vacuum chamber at 20–30 kV accelerating voltage to capture the images. The fibers were characterized for the mean diameter using the ImageJ software and a histogram of diameter distribution was plotted for 50 independent measurements.

#### Fourier Transform Infrared Spectroscopy (FTIR)

For FTIR analysis, the drug powder, polymers, and nanofibers were ground with potassium bromide powder and then were compressed into tablets using a manual compressing machine under 10 tons of pressure for 15 min. The spectra of samples were generated by an IR prestige-21 (Shimadzu, Japan) spectrophotometer in a wavenumber range between 4000 and 400 $cm^{-1}$.

#### Swelling, Moisture Loss, and Uptake

The swelling percentage of nanofibers was examined by immersing them in phosphate buffer solution (PBS) at a pH of 7.4 for 24 h. At 24-h intervals, the nanofibers were weighed after the elimination of surface water by placing them between sheets of filter paper. The swelling was determined using Eq. 1.

$$\text{Swelling } (\%) = \frac{W_{\text{Final}} - W_{\text{Initial}}}{W_{\text{Initial}}} \times 100 \quad (1)$$

$W_{\text{Final}}$ stands for the weight of samples after the examination and $W_{\text{Initial}}$ stands for the weight of samples before the examination.

Generally, nanofibers should have an appropriate level of stability in dry and humid conditions to preserve their properties while being exposed to different relative humidity (RH). To determine the stability of nanofibers, dry and humid conditions were simulated in enclosed containers using $CaCl_2$ and $AlCl_3$ (RH = 79.5%). The pre-weighed samples were placed in containers and after 3 days the samples were reweighed. The changes in the weight of samples were

recorded, and then the moisture loss and moisture uptake were calculated by Eqs. 2 and 3.

$$\text{Moisture uptake } (\%) = \frac{W_{\text{Final}} - W_{\text{Initial}}}{W_{\text{Initial}}} \times 100 \quad (2)$$

$$\text{Moisture loss}(\%) = \frac{W_{\text{Initial}} - W_{\text{Final}}}{W_{\text{Initial}}} \times 100 \quad (3)$$

$W_{\text{Initial}}$ stands for the weight of samples before examination and $W_{\text{Final}}$ stands for the weight of samples after examination. The tests were performed in triplicate.

### Encapsulation Efficiency (EE%)

Nanofibers with specific weights were dissolved in proper solvent systems (distilled water for PVA, acetic acid (1% v/v) for CS, and DCM/DMF/ACT (4:5:1 v/v) for PCL) and then were examined for ultraviolet (UV) absorbance at a maximum wavelength of 365 nm using a UV mini-1240 UV-visible spectrophotometer (Shimadzu, Japan). The EE% was calculated by Eq. 4, where $W_M$ stands for the weight of the measured drug in nanofibers, and $W_U$ stands for the weight of the drug used in the preparation of nanofibers. The test was repeated for 3 samples and a mean value was reported.

$$\text{EE}(\%) = \frac{W_M}{W_U} \times 100 \quad (4)$$

### Tensile Testing

An STM-5 testing machine (Santam, Iran) was utilized to investigate the tensile strength and flexibility of nanofibers. For this aim, nanofibers were cut into $3 \times 1$ cm$^2$ rectangular pieces and fixed between two grips of the machine. The upper moving grip moved upward at the constant rate of 1 mm/min until the sample was torn. Grip distance and maximum pulling force in heading tensile testing were 20 mm and 900 N, respectively. The maximum resisted stress at peak and the elongation percentage at break were measured for each sample ($n = 3$). Moreover, the stress-strain curve was constructed to estimate the elasticity behaviour of nanofibers.

### Water Contact Angle

A self-assembled device including a Dino-Lite AM7815 digital microscope (AnMo Electronics Corp, Taiwan) fixed at a horizontal position, was utilized to perform the test. Samples of nanofibers were placed in the testing chamber followed by the addition of one drop of distilled water trickled on the surface of the sample. The camera captured images at a rate of 2 frame/s and the captured images were evaluated to determine the water contact angle using Image software.

## Stability Studies

The stability of the optimized formulation (PVA-PCL-CS) was assessed in accordance with ICH guidelines. The formulation was stored at a controlled temperature of $25 \pm 2$°C and relative humidity (RH) of $60 \pm 5$% for 12 months. At 3-, 6-, and 12-month intervals, various parameters were evaluated to monitor any changes from the baseline.

The parameters assessed during the stability study included the encapsulation efficiency (EE%), the morphology of the fibers, the diameter of the fibers, and the tensile strength. By conducting these evaluations at regular intervals, the study aimed to determine if there were any alterations in the characteristics and performance of the formulation over time.

## *In Vitro* Antimicrobial Efficacy Against Periodontal Pathogens

The antimicrobial efficacy of nanofibers was evaluated by determining the inhibition growth zones against four of the most common pathogens that are responsible for severe forms of periodontitis, i.e. *A. actinomycetemcomitans* (*ATCC 33384*), *A. viscosus* (*ATCC 19246*), *P. intermedia* (*ATCC 25611*), and *P. gingivalis* (*ATCC 33277*). The species were inoculated on TSA plates and incubated at $37 \pm 1$°C in an anaerobic jar. Anaerobic conditions were provided using Anaerocult®-A gas packs. After 24 h of incubation, 0.5 McFarland bacterial suspension of species in PBS was prepared and spread in 6 directions on TSA plates. Nanofibers were cut into pieces with specific weights (same amount DOX) and placed onto the inoculated plates. After 24 h of incubation at $37 \pm 1$°C in an anaerobic condition, the diameter of inhibited growth zones was measured for nanofibers against each species. The test was performed in triplicate and an average was taken.

## *In Vitro* Cell Toxicity

MTT assay was carried out to evaluate the toxicity of DOX-loaded GTR membranes on L929 mouse fibroblast cells (Pasteur Institute, Tehran, Iran). The cells were cultured in a 96-well plate along with DMEM containing 10% FBS, 100 U/mL penicillin, and 100 µg/mL streptomycin at $37 \pm 0.5$°C and an atmosphere containing 5% $CO_2$ for 24 h. Pieces of GTR membranes containing different amounts of DOX (previously exposed to UV radiation for the elimination of surface contamination) were immersed in 1 mL of DMEM to achieve DOX concentrations of 100, 50, 25, and 12.5 µg/mL and incubated at $37 \pm 0.5$°C for 48 h. The supernatant of samples soaked in

DMEM was transferred to the 96-well plate for cell contact and incubated for another 24 h. Control was developed as well in a row that did not receive any formulation. Finally, 10 µL of MTT solution (5 mg/mL) and trypsin were added to the wells of the plate, and it was incubated for another 4 h at 37 ± 0.5°C. The absorbance of samples at 570 nm was measured by a spectrophotometer and the cell viability was calculated by dividing the sample absorbance by control absorbance. Blank samples were also examined by MTT assay.

## *In Vitro* Release Study

Each formulation (25 mg) was put in a cellulose dialysis membrane with a cut-off pore size of 12,000 Daltons, then enclosed and immersed as a donor compartment in 25 mL of PBS medium at 37 ± 0.5°C under 100 rpm agitation. Sampling was conducted at regular intervals, and after withdrawing aliquots, the medium was replaced with fresh PBS to maintain a sink condition. The amount of DOX released was determined by UV spectroscopy (UV-Mini1240, Shimadzu, China) at a maximum wavelength of 365 nm. The test was performed in triplicate. The release data were fitted to different kinetical models (zero-order, first-order, Higuchi, and Korsemeyer-Pappas) and the model indicated the highest $R^2$ value and the lowest mean percentage error (MPE) was selected as the best-fitted model.

## Sterility Testing

Before the animal study, the membranes were analyzed for sterility to avoid unwanted infection at the site of administration. Glass tubes containing TSB, FTM, and SDB were autoclaved at 121°C for 15 min. Pieces of blank and drug-loaded membranes were exposed to UV radiation (365 nm) for 10 min to eliminate possible surface contamination, followed by immersion in the prepared culture media [25]. Positive control was developed by inoculation of *Escherichia coli* (ATCC: 25922) in TSB, *Bacillus subtilis* (ATCC: 21332) in FTM, and *Candida albicans* (PFCC: 62194) in SDB. Tubes that did not receive any samples and microorganisms were considered negative controls. The TSB, FTM, and SDB tubes containing samples were observed for 28 days of incubation at appropriate conditions for any sign of turbidity comparable to positive control to detect any contamination with aerobic bacteria, anaerobic bacteria and fungi, respectively.

## Animal Studies

### *In Vivo* Implantation in Rat

All animal experiments were approved by the Local Ethical Committee of Kermanshah University of Medical Sciences; approval number: IR.KUMS.REC.1400.519. Investigations followed the guidelines articulated in the Declaration of Helsinki and its Guiding Principles in the Care and Use of Animals (NIH Publication No. 85–23, 1987 revision). *In vivo* evaluation in rats was performed using a replacement method that has been developed to overcome the challenges related to the small size of the oral cavity in most animal models. Apart from some microscopic differences, as cutaneous and gingival tissues possessed similar patterns of hemostasis, inflammation, proliferation, and remodelling of the collagen [26], thus, to evaluate the biocompatibility and therapeutic performance of the membranes, the obtained membranes were implanted in the subcutaneous tissues of the dorsal part of a rat model. This method has been used previously for the evaluation of GTR membranes in similar studies [27, 28].

To perform the animal study, 27 healthy Wister rats weighing 200–400 g that were housed under standard conditions were anaesthetized by intraperitoneal injections of ketamine (10 mg/kg). Then, implantation pockets were cut in the shaved dorsal skin of rats using a sterile scalpel blade. Pieces of the PVA-PCL-CS DOX-loaded GTR membrane (25 mg) were implanted into the pockets and they were closed by sutures. The samples were taken out at specific time intervals within 3 weeks of implantation and washed with PBS. The residual DOX in each piece was quantified using UV spectroscopy after the dissolution of the explanted sample in the proper solvent including distilled water for PVA, acetic acid (1% v/v) for CS, and DCM/DMF/ACT (4:5:1 v/v) for PCL. The amount of drug released and absorbed by the surrounding tissue was measured by subtracting the residual drug from the total drug content of the membrane. The rats were euthanized according to the ethical guidelines at the end of the procedure.

### Histopathological Biocompatibility Study

The samples were implanted in rats according to the method enclosed in "*In vivo* Implantation in Rat" section. Tissue samples were collected at specific time intervals and fixed in formalin for 24 h. The samples were dehydrated by utilizing an ethanol solution, then paraffined, cut, and coloured with hematoxylin and eosin. The prepared slides were observed and imaged by a light microscope and evaluated for signs of inflammation and damage by a pathologist. The biocompatibility of membranes was discussed based on the histopathological findings.

## Statistical Analysis

To compare the results, one-way ANOVA and the post hoc Tuckey's tests were performed for a significance level of 0.05 using SPSS software (version 25.00).

## Results and Discussion

### Physicochemical Characterization DOX-Loaded GTR Membranes

At the moment, oral antibiotics are used to treat periodontitis. However, these antibiotics have systemic adverse effects and have not been able to reach therapeutic concentrations (above minimum inhibitory concentrations, or MIC) in the periodontal pocket [29]. To effectively treat periodontitis without causing systemic side effects, the current study investigated the use of the GTR system to extend the drug release in the periodontal pocket. Using GTR systems for the treatment of periodontitis has several benefits. GTR stops connective tissue from obstructing osteogenesis and penetrating the region of bone reformation. Additionally, it makes an area beneath the surgical flap that serves as a scaffold for the development of blood vessels and cells. GTR can maintain the mechanical stability of the healing complex, separate regeneration space from undesired tissues, and guard against bacterial invasion, which stops the host immune system's inflammatory reaction [30].

For the GTR membrane to work well as a barrier membrane, it needs to possess several characteristics. These qualities consist of biocompatibility, safety, non-allergic, non-toxic, and mechanical stability [9, 31–33].

#### SEM Studies

Figure 1 represents the SEM images of developed GTR membranes. The mean diameter of $445 \pm 43$ nm and $408 \pm 43$ nm was estimated for PVA-PCL-CS and PVA-PCL formulations. The mean diameter of nanofibers in the submicron range would lead to a high surface-to-volume ratio that can modify the release rate and enhance drug delivery [34]. Electrospun nanofibers, configured as nanomats, possess two key attributes that make them appealing as drug carriers. Firstly, their already substantial surface area-to-volume ratio is further amplified by considering the porosity of the electrospun nanofibers. This increased surface area addresses the challenge of high drug uptake commonly associated with traditional systems. Additionally, it overcomes the limitation of drug diffusion by virtue of its high surface area and interconnected porous structure, resulting in a higher fraction of drug released overall. Secondly, the properties of the nanofiber, such as the fiber's diameter, porosity, and morphology, can be controlled and customized by varying the processing parameters and the material type. These properties affect the drug release profile from the nanofiber and physicochemical properties.

It can be seen from the SEM images (Fig. 1) that the obtained electrospun nanofibers have uniform nanofibrous structures with random alignment. The addition of CS to the formulation did not cause a significant change in the mean diameter of the formulation ($p < 0.05$). In a similar study, co-axial PVA-PCL nanofibers were developed as wound dressing by electrospinning, which indicated mean diameter values in a range between 400 and 600 nm [35]. The porous structure of nanofibers makes them suitable as a scaffold for cell growth as their pore size is much smaller than the size of fibroblast cells; therefore, the cells cannot penetrate through the nanofibrous membrane [36].

#### FTIR Studies

Figure 2 displays the FTIR spectra of polymers, the drug, and the developed GTR membranes. The spectrum of pure DOX shows a characteristic broad peak at 3423 $cm^{-1}$ assigned to N-H and OH stretching. Peaks at 3107, 1774, 1527, 1247, and 1033 $cm^{-1}$ are attributed to aromatic C-H, C = O, amide band, C-C-C, and -C-N stretching, respectively. A peak at 938 $cm^{-1}$ appears in the spectrum of DOX indicating the out-of-plane bending of ring C–H bonds [37]. The shift of the C-C-C peak in nanofiber formulations at 1240 $cm^{-1}$, and also the -C-N peak at 1045 and 1049 $cm^{-1}$ confirmed the presence of DOX inside the PVA-PCL and PVA-PCL-CS nanofiber structure, respectively. Pure PVA indicates a peak at 3414 $cm^{-1}$ related to OH stretching. A peak at 1722 $cm^{-1}$ appears in the spectrum of pure PCL assigned to C = O stretching. Also, peaks at almost 2900, 2800, and 1100 $cm^{-1}$ appear in the spectra of both PVA and PCL polymers attributed to asymmetrical C-H, symmetrical C-H, and C-O/C-O-C stretching, respectively [38]. Pure chitosan indicates a broad peak at 3400 $cm^{-1}$ related to OH and NH stretching vibrations and two peaks at 1654 and 1597 $cm^{-1}$ assigned to acetyl and NH2 groups [39]. The PVA-PCL-CS nanofiber showed a higher intensity of the peak at 3400 $cm^{-1}$ compared to PVA-PCL nanofiber as it contains CS with OH and NH groups at multiple positions.

The FTIR spectrum of nanofibers (Fig. 2) indicated some characteristic peaks of the drug and polymers with negligible changes in frequency or intensity. Consequently, no interaction occurred between the pharmacologically active moiety of the drug and polymers, hence drug-polymer compatibility.

#### Swelling, Moisture Loss, and Uptake

The swelling characteristic of a nanofiber could play an important role in the determination of release behaviour. The swelling data for various formulations are shown in Table I. A slightly lower degree of swelling was obtained for PVA-PCL-CS ($214.1 \pm 7.0\%$) compared to the PVA-PCL membrane ($220.3 \pm 11.4\%$). This lower swelling could be due to

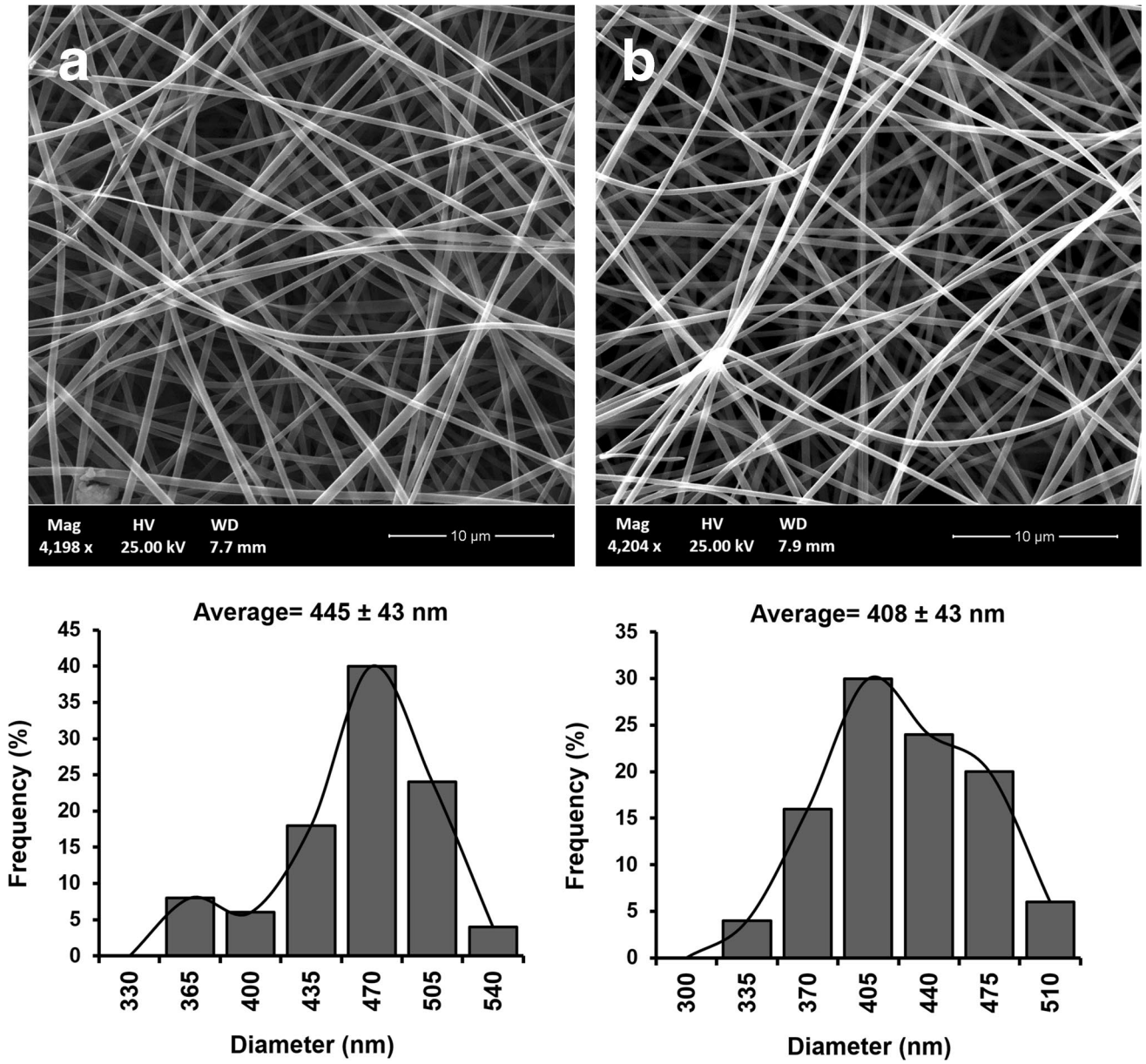


**Fig. 1** SEM images of developed PVA-PCL-CS (**a**) and PVA-PCL (**b**) GTR membranes along with the plotted histograms of size distribution

the insolubility of CS in water. However, the difference in swelling was not statistically significant ($p > 0.05$). Previous studies reported decreased swelling by increasing the CS content [40]. The formulation showed suitable stability at different humidity degrees between $0.4 \pm 0.1$ and $1.3 \pm 0.3$ as less than 2% of weight changes were observed in dry and humid conditions.

### Encapsulation Efficiency

The encapsulation efficiency percentage (EE%) results for both formulations are listed in Table I and the results showed that both formulations showed EE% of above 97% ($97.8 \pm 1.2$–$98.1 \pm 1.0$). Electrospinning is the most efficient method for the preparation of drug-loaded nanofibers [41]. The passive drug loading technique, which involves incorporating the therapeutic agent into the polymeric solution before spinning, is responsible for achieving a higher entrapment efficacy. However, there is a slight reduction in entrapment efficiency. This may be attributed to the diminishing drainage capacity of the collector as the fibers accumulate on its surface, causing some fibers to be diverted away from the collector site. The high drug loading could be an advantage as a high dose of the drug can be loaded in less bulky dosage forms [42].

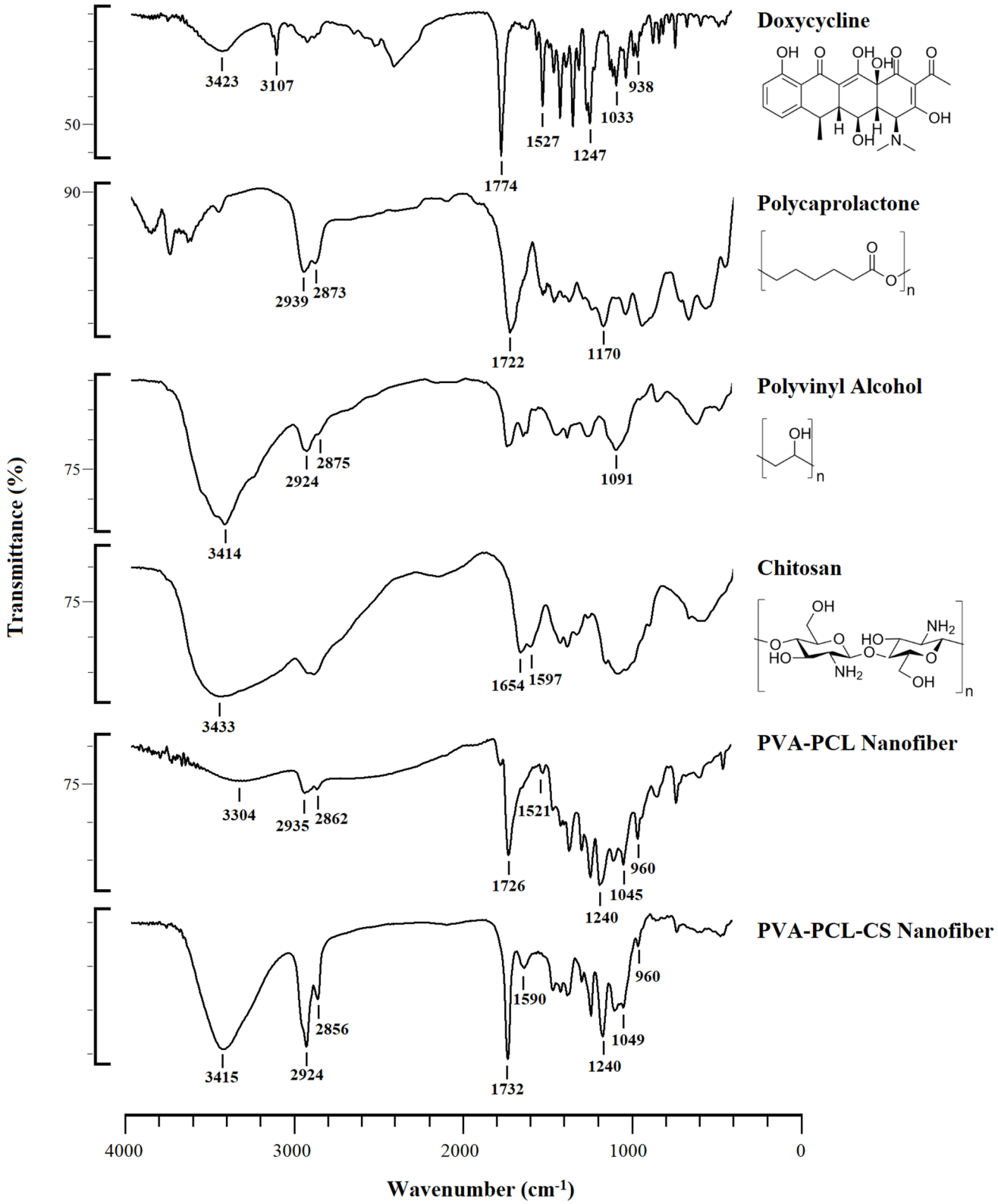


**Fig. 2** FTIR spectra of DOX, PCL, PVA, CS, and developed PVA-PCL-CS and PVA-PCL GTR membranes

**Table I** Physicochemical Characteristics of Developed DOX-Loaded GTR Membranes

| Formulation | Swelling (%) | Moisture loss (%) | Moisture uptake (%) | EE (%) | Tensile strength (MPa) | Elongation at break (%) |
|---|---|---|---|---|---|---|
| PVA-PCL | 220.3 ± 11.4 | 1.3 ± 0.3 | 0.8 ± 0.4 | 98.1 ± 1.0 | 2.71 ± 0.12 | 34.48 ± 3.82 |
| PVA-PCL-CS | 214.1 ± 7.0 | 0.4 ± 0.1 | 0.5 ± 0.2 | 97.8 ± 1.2 | 2.17 ± 0.55 | 22.81 ± 5.35 |

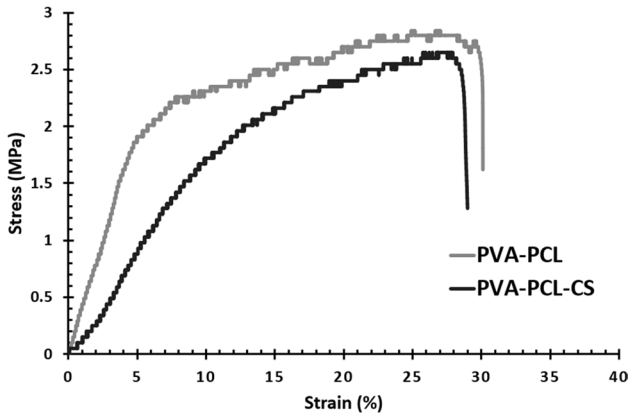


**Fig. 3** Stress-strain curve obtained for DOX-loaded GTR membranes through tensile testing

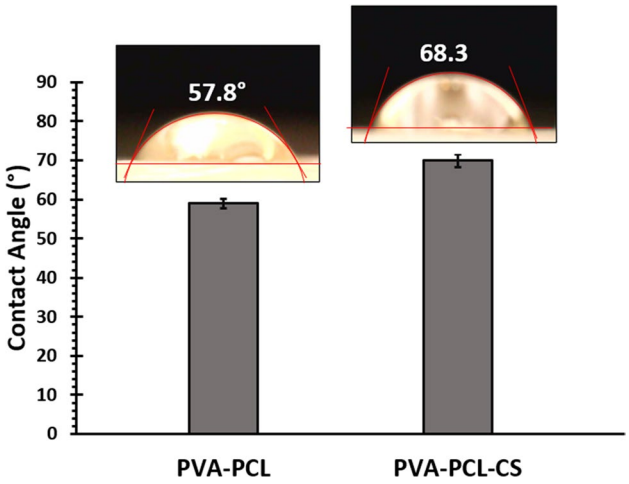


**Fig. 4** Water contact angles of DOX-loaded GTR membranes

### Tensile Testing

The tensile strength indicates the resistance of the nanofibers against an external force when placed between two clamps. Figure 3 indicates the stress-strain curves obtained for DOX-loaded nanofiber. The stress-strain curve (Fig. 3) followed a behaviour similar to elastic materials which was similar to the study carried out by Taghe *et al*., where they developed PCL-PVA formulations with similar results [43]. The results exhibited that PCL-PVA had higher elongation at break (34.48 ± 3.82%) compared to PCL-PVA-CS (22.81 ± 5.35%) and the difference in tensile strength is statistically significant ($p < 0.05$). According to a previous study, the tough and stiff nature of CS with higher molecular weight could be the reason behind the reduced flexibility [44]. Both formulations showed appropriate tensile strength (> 2 MPa) and elongation (> 20%) which can be considered high strength and flexible membranes, thus suitable for handling and placing in the periodontal pocket [45].

### Water Contact Angle

The water contact angle is an indicator of the surface hydrophilicity of nanofibers. Figure 4 displays the mean water contact angle of formulations. PCL-PVA showed a mean contact angle of 57.8 ± 1.1° while PVA-PCL-CS showed a mean value of 68.3 ± 1.6°. The slightly higher water contact angle of PVA-PCL-CS compared to PCL-PVA could be due to increased surface hydrophobicity of the membrane when CS (a water-insoluble molecule) existed in the membrane [40].

Notably, both formulations showed appropriate surface hydrophilicity to be fixed in the periodontal pocket and allow the cells to grow on the membranes as scaffolds by indicating less than 90° of contact angle. It has been reported that as PVA nanofibers were hydrophilic, they showed a contact angle of around 35° [46] while in the case of PCL nanofibers (hydrophobic), this value was 128° [47]. The current results showed that by blending these two polymers it was possible to fabricate fibers with a desirable contact angle.

### *In Vitro* Antimicrobial Efficacy Against Periodontal Pathogens

The antimicrobial efficacy of the formulation against four common periodontal pathogens was investigated (Fig. 5). Table II represents the mean diameter of inhibited growth zones against different pathogens. All formulations showed significant antimicrobial effects with inhibited growth zones of 27.8 ± 1.1–33.9 ± 0.3 mm for PVA-PCL and 30.7 ± 1.1–38.1 ± 0.8 mm for PVA-PCL-CS. Clearly, PVA-PCL-CS showed a higher diameter of inhibited growth zones compared to PVA-PCL due to the antimicrobial effect of CS. Many studies confirmed that CS has antibacterial effects on common periodontal pathogens [21, 48, 49]. The highest diameter of inhibited growth zones was obtained against *A. actinomycetemcomitans* for both formulations.

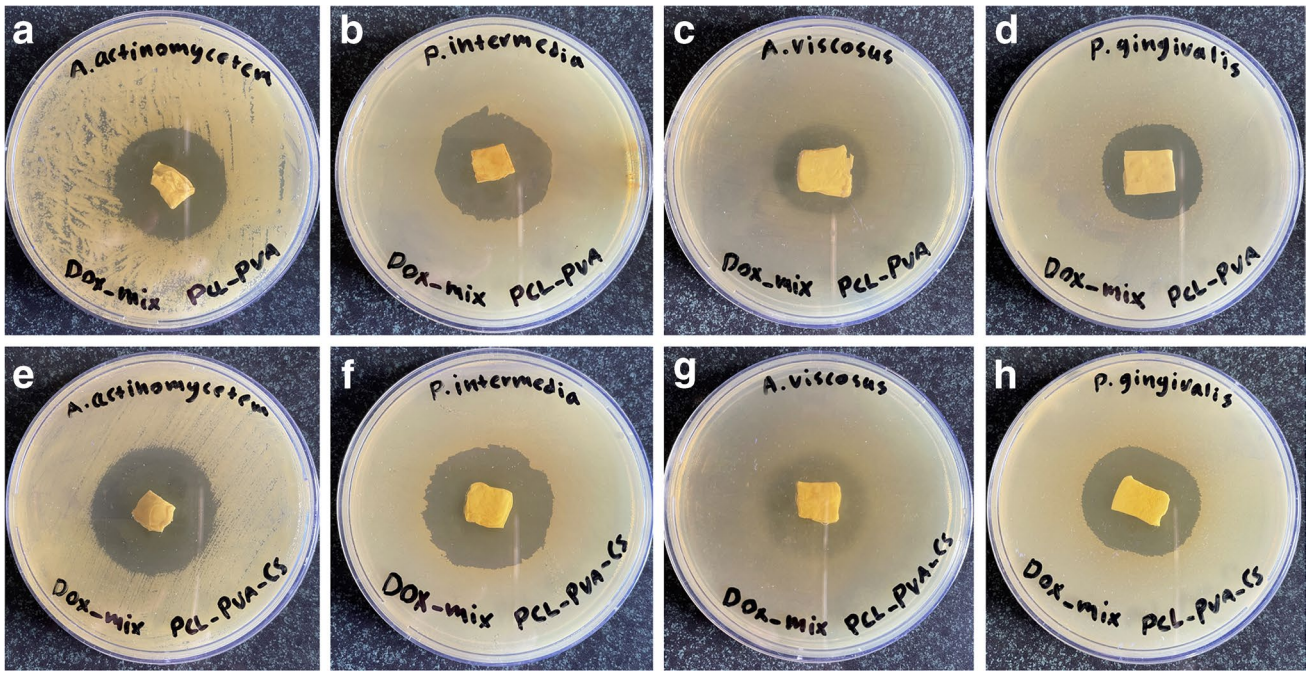


**Fig. 5** Inhibited growth zones obtained for PCL-PVA and PCL-PVA-CS DOX-loaded GTR membranes against *A. actinomycetemcomitans* (**a**, **e**), *P. intermedia* (**b**, **f**), *A. viscosus* (**c**, **g**), and *P. gingivalis* (**d**, **h**)

## *In Vitro* Cell Toxicity

Figure 6 indicates the cell viability obtained after exposure of cells to different formulations during the MTT assay. The cell toxicity results (Fig. 6) showed that an increase in DOX concentration led to a decreased cell viability as blank formulations (free of drug) indicated the lowest level of cell toxicity with more than 93% cell viability within 48 h of incubation. More than 78% of cell viability was obtained for both formulations even at 1000 µg/mL concentration of the drug during the first 24 h indicating the non-toxicity of formulations [50]. The PVA-PCL-CS showed slightly higher toxicity compared to PVA-PCL at almost all drug concentrations used during 72 h of investigation which could be due to the presence of CS in the formulation [51]. Such a behaviour has been concluded in a previous study [52] but still needs further investigation.

The cell viability decreased as time progressed from 24 to 72 h for both formulations but did not drop lower than 70% for the longest time (72 h) studied. The PVA-PCL and PVA-PCL-CS formulations indicated 73.68 ± 6.00% and 72.36 ± 1.48% of cell viability at 1000 µg/mL of the drug concentration during 72 h of examination. Accordingly, both formulations can be considered safe to be used as a GTR membrane.

**Table II** The Mean Diameter of Inhibited Growth Zones Against Periodontal Pathogens Obtained by DOX-Loaded GTR Membranes

| Formulation | Mean diameter of inhibited growth zone (mm) | | | |
|---|---|---|---|---|
| | *A. actinomycetemcomitans* | *P. intermedia* | *A. viscosus* | *P. gingivalis* |
| PVA-PCL | 33.9 ± 0.3 | 33.5 ± 1.9 | 27.8 ± 1.1 | 30.1 ± 0.7 |
| PVA-PCL-CS | 38.1 ± 0.8 | 36.8 ± 1.4 | 30.7 ± 1.1 | 32.5 ± 2.7 |

## *In Vitro* Release Study

The results of the *in vitro* release study showed a controlled release of DOX from both drug-loaded GTR membranes (Fig. 7). PVA-PCL and PVA-PCL-CS released 77.81 ± 2.61% and 48.49 ± 0.97% of their drug content within the first 10 h of the study respectively. The formulation released 70–90% of its drug content during an extended period of 30 h. The low drug release rate for formulations containing CS compared to the formulation without CS could be due to the higher hydrophobicity and lower degree of swelling of PVA-PCL-CS compared to PVA-PCL where there is no CS in the formulation. In a study conducted by Jia *et al*., it was shown that approximately 50% DOX was released from PCL-based nanofibers during the first day [53]. Additionally, a 2-week tetracycline release was reported from PVA/CS nanofibrous GTR membrane

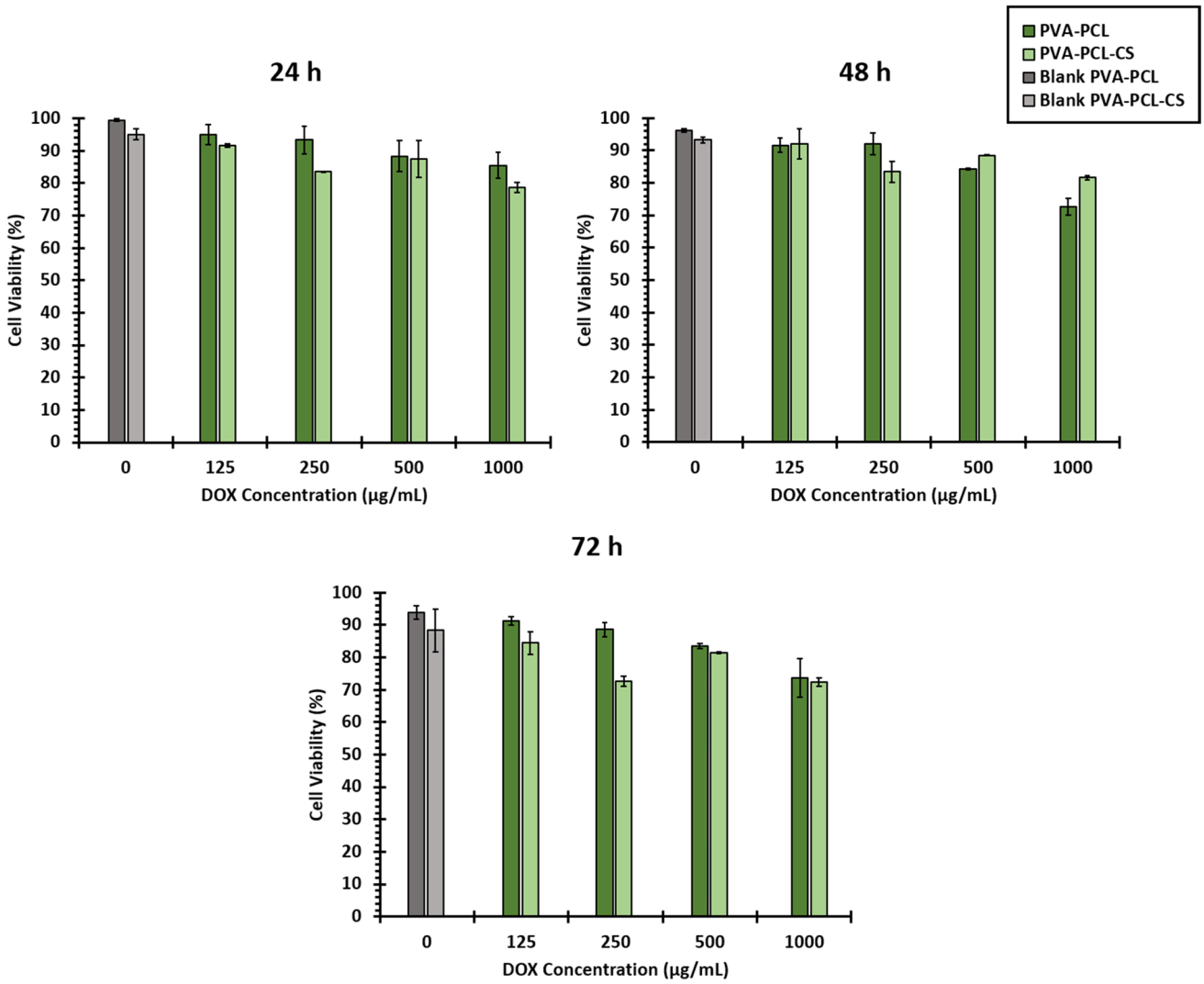


**Fig. 6** Cell viability of L929 fibroblasts after exposure to DOX-loaded and blank GTR membranes during MTT assay at different intervals

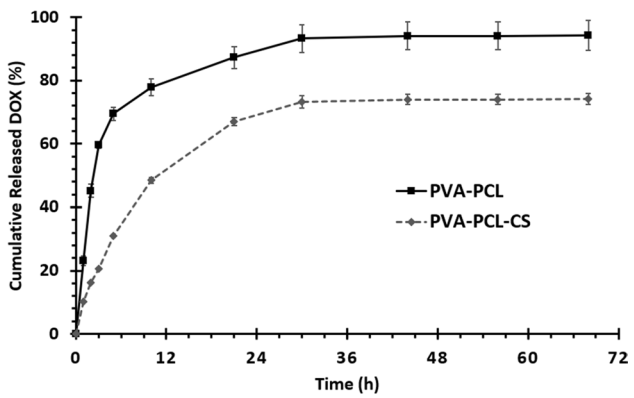


**Fig. 7** *In vitro* release profile of DOX from the developed GTR membranes in PBS

based on core-sheath electrospun nanofibrous nonwovens crosslinked upon immersion in genipin ethanolic solution [20]. Other studies based on CS formulations showed 136-h release in the case of minocycline [54] and 200 h in the case of tetracycline [55].

As mentioned earlier in the "In vitro release study" section, the release data were also fitted to various kinetic models and the results in Table III showed that the best-fitted kinetic model for both formulations was the Peppas and Korsmeyer model (Eq. 4) where $r^2$ values were much higher than the other kinetics models (0.993–0.998). In addition, the mean percentage errors (MPE%) for the Peppas-Korsemeyer model were much lower than other kinetic models. Based on the *n* values reported in Table III, the main mechanism for PVA-PCL was diffusion as the *n* value is closer to 0.5, but when CS was added to the formulation the *n* value increased to 0.76 which indicates that the main mechanism

**Table III** $R^2$ Values Were Obtained by Fitting the Release Data of Formulations in Different Kinetical Models

| Formulation | Zero-order | | First-order | | Higuchi | | Korsemey-Peppas | | |
|---|---|---|---|---|---|---|---|---|---|
| | $R^2$ | MPE (%) | $R^2$ | MPE (%) | $R^2$ | MPE (%) | $R^2$ | MPE (%) | $n$ |
| PVA-PCL | 0.727 | 38 | 0.775 | 39 | 0.878 | 22 | 0.993 | 5 | 0.61 |
| PVA-PCL-CS | 0.596 | 24 | 0.741 | 22 | 0.760 | 18 | 0.998 | 1.2 | 0.76 |

of the drug release is the combination of diffusion and erosion ($n$ closer to 1 is an indication of erosion mechanism). In the Korsemeyer-Peppas equation (Eq. 5), $Mt/M\infty$ is the fraction of the released drug at time $t$, $K$ is the release rate constant, and $n$ is the release exponent (mechanism of drug release).

$$M_t/M_\infty = Kt^n \tag{5}$$

## Animal Studies

### *In Vivo* Implantation in Rat

Blank and drug-loaded nanofibers of both formulations showed sterility as the whole preparation procedure was performed under aseptic conditions. No significant turbidity was observed in any of the test tubes indicating the sterility of formulations and suitability of the made membranes for *in vivo* evaluation.

The subcutaneously implanted membranes of PVA-PCL-CS DOX-loaded GTR in rates exhibited a controlled release pattern for the drug for 2 weeks to the surrounding tissues. Figure 8a represents the rate of drug release into the nearby tissues. For *in vivo* studies, the highest rate of drug release was achieved on the first day of implantation ($2444.5 \pm 75.9$ µg/day); then, the rate of release decreased during the following 14 days (Fig. 8). This indicates that there was an initial burst drug release for approximately 40% of the drug payload within the first 24 h, followed by steadily decreasing drug release. Similar results were reported by Mirzaeei *et al*., where subcutaneous implantation of metronidazole-amoxicillin-loaded GTR membranes in the dorsal area of rats led to a 14-day release of the drug [56], and another study minocycline hydrochloride–loaded nanofibrous membranes the *in vivo* evaluation indicated a prolonged release of minocycline for 15 days [56]. It is believed that due to the slower wash-out rate of the drug from the tissue compared to *in vitro* conditions, a more gradual release was observed *in vivo*.

### Histopathological Biocompatibility Study

Figure 8b displays the histopathological findings of the biocompatibility study. In the image of samples collected on day 7, inflammatory cells (e.g. lymphocytes and neutrophils) are clearly detectable indicating a severe inflammation at the implantation site. This refers to the anticipated tissue reaction following encountering a foreign body invasion or occurrence of tissue injury. The number of these inflammatory cells reduced on day 14 (moderate inflammation) and day 21 (mild inflammation) due to a decrease in general predictable tissue reaction [57].

Histopathological biocompatibility result (Fig. 8b) indicates that although inflammation could occur in the initial days of the administration, it would alleviate the inflammation in later days as discussed above. Mirzaeei *et al*. reported similar results for amoxicillin/metronidazole-loaded GTR membranes [56]. No tissue damage is detectable at the implantation site showing the biocompatibility of the DOX-loaded GTR membrane.

## Stability Studies

Stability testing is a crucial step in ensuring the quality and efficacy of pharmaceutical products. The data obtained from this study would provide valuable insights into the long-term stability of the PVA-PCL-CS formulation, aiding in its potential development as a reliable and effective drug delivery system. Table IV represents the parameters obtained in stability testing. The optimized formulation (PVA-PCL-CS) showed long-term stability during the 12-month stability study as no significant changes were observed in the physicochemical characteristics of the fibers ($P > 0.05$). A similar study indicated long-term stability at ambient conditions for DOX-loaded PCL/CS/alginate nanofibers as wound dressings and instability at higher humidity [58]. Further studies under accelerated conditions are required to discuss the stability of the membrane.

## Conclusion

Dual function–guided tissue regeneration membranes with both space-maintaining regenerative function and controlled drug delivery capability were recently developed. These systems can accelerate the healing process of tissues surrounding a tooth affected with periodontitis, by releasing drugs adjacent to guided tissue regeneration along with forming a space for cell growth and differentiation. The present work developed doxycycline-loaded membranes using blends of polycaprolactone/polyvinyl alcohol/chitosan polymers. The

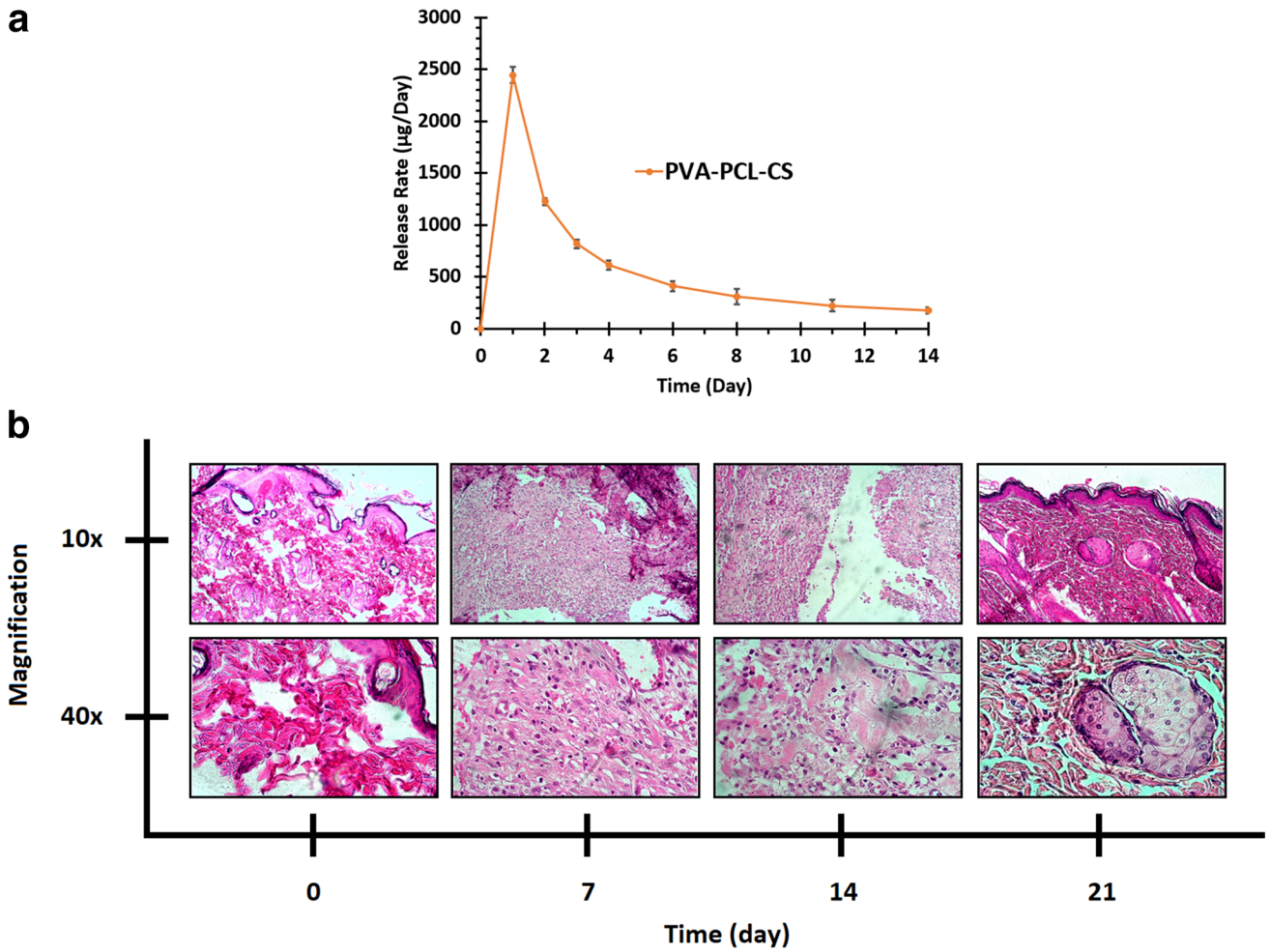


**Fig. 8** The rate of drug release from DOX-loaded GTR membrane (PVA-PCL-CS) after subcutaneous implantation in the dorsal skin of rat (**a**) and the histopathological images of surrounding tissues during days 0, 7, 14, and 21 of biocompatibility study (**b**)

**Table IV** Stability Test Parameters Obtained for PVA-PCL-CS DOX-Loaded GTR Nanofiber

| Timepoint (months) | Mean fiber diameter (nm) | EE (%) | Tensile strength (MPa) | Morphology |
|---|---|---|---|---|
| 3 | 481 ± 52 | 96.3 ± 2.6 | 2.33 ± 0.71 | Randomly aligned uniform nanofibers |
| 6 | 473 ± 49 | 95.9 ± 1.5 | 2.62 ± 0.23 | Randomly aligned uniform nanofibers |
| 12 | 495 ± 32 | 95.1 ± 2.1 | 2.49 ± 0.58 | Randomly aligned uniform nanofibers |

membranes possessed appropriate stability, surface hydrophilicity, strength, and flexibility which made them suitable as a guided tissue regeneration membrane with a space-maintaining function. Also, a prolonged *in vitro* release was observed for the formulations. The formulations showed inhibited growth zones of more than 20 mm against four major anaerobic pathogens in periodontitis while being non-toxic to fibroblast cells. *In vivo* evaluation showed extended release of the drug after subcutaneous implantation in rats' dorsal skin for 14 days and histopathological examinations showed acceptable biocompatibility for membranes. Owing to these beneficial effects, the doxycycline-loaded guided tissue regeneration membranes can be considered a suitable replacement for blank membranes to achieve a therapeutic concentration of drug at the affected site while preserving a regenerative function.

**Acknowledgements** We sincerely thank Rahesh Daru Novine, Pharmaceutical Sciences Research Center, for their cooperation in providing materials and equipment.

**Author Contribution** S. M.: conceptualization, methodology, validation, formal analysis, investigation, resources, data curation,

writing—review and editing, visualization, supervision, project administration, funding acquisition; S. P.: methodology, software, formal analysis, investigation, data curation, visualization; M. S.: software, formal analysis, investigation, writing—original draft; A. N.: validation, writing—review and editing; S. T.: software, formal analysis, investigation.

**Funding** This research was funded by the Research Council of Kermanshah University of Medical Sciences (Grant number: 4000660).

**Data Availability** The data will be available on request.

## Declarations

**Conflict of Interest** The authors declare no competing interests.

**Institutional Review Board** The animal study protocol was approved by the Local Ethical Committee of Kermanshah University of Medical Sciences; approval number: IR.KUMS.REC.1400.519.



## References

1. Laine ML, Crielaard W, Loos BG. Genetic susceptibility to periodontitis. Periodontol. 2000;2012(58):37–68.
2. Mehrotra N, Singh S. Periodontitis. Treasure Island (FL): StatPearls Publishing; 2023. https://www.ncbi.nlm.nih.gov/books/NBK541126.
3. Eke PI, Page RC, Wei L, Thornton-Evans G, Genco RJ. Update of the case definitions for population-based surveillance of periodontitis. J Periodontol. 2012;83:1449–54.
4. Richards D. Review finds that severe periodontitis affects 11% of the world population. Evid Based Dent. 2014;15:70–1.
5. Needleman I, Tucker R, Giedrys-Leeper E, Worthington H. A systematic review of guided tissue regeneration for periodontal infrabony defects. J Periodontal Res. 2002;37:380–8.
6. Chen S, Hao Y, Cui W, Chang J, Zhou Y. Biodegradable electrospun PLLA/chitosan membrane as guided tissue regeneration membrane for treating periodontitis. J Mater Sci. 2013;48:6567–77.
7. Lin L, Chen MY, Ricucci D, Rosenberg PA. Guided tissue regeneration in periapical surgery. J Endod. 2010;36:618–25.
8. Hurley LA, Stinchfield FE, Bassett CAL, Lyon WH. The role of soft tissues in osteogenesis: an experimental study of canine spine fusions. JBJS. 1959;41:1243–66.
9. Wang J, Wang L, Zhou Z, Lai H, Xu P, Liao L, Wei J. Biodegradable polymer membranes applied in guided bone/tissue regeneration: a review. Polymers. 2016;8:115.
10. Kajiya M, Giro G, Taubman MA, Han X, Mayer MP, Kawai T. Role of periodontal pathogenic bacteria in RANKLmediated bone destruction in periodontal disease. J Oral Microbiol. 2010;2(1):5532.
11. Pérez-Chaparro PJ, Gonçalves C, Figueiredo LC, Faveri M, Lobão E, Tamashiro N, Duarte P, Feres M. Newly identified pathogens associated with periodontitis: a systematic review. J Dent Res. 2014;93:846–58.
12. Jepsen K, Jepsen S. Antibiotics/antimicrobials: systemic and local administration in the therapy of mild to moderately advanced periodontitis. Periodontology. 2000;2016(71):82–112.
13. Slots J, Rams TE. Antibiotics in periodontal therapy: advantages and disadvantages*. J Clin Periodontol. 1990;17:479–93.
14. Mirzaeei S, Ezzati A, Mehrandish S, Asare-Addo K, Nokhodchi A. An overview of guided tissue regeneration (GTR) systems designed and developed as drug carriers for management of periodontitis. J Drug Deliv Sci Technol. 2022;71: 103341.
15. Carter P, Rahman SM, Bhattarai N. Facile fabrication of aloe vera containing PCL nanofibers for barrier membrane application. J Biomater Sci Polym Ed. 2016;27:692–708.
16. Mehrandish S, Mirzaeei S. A review on ocular novel drug delivery systems of antifungal drugs: functional evaluation and comparison of conventional and novel dosage forms. Adv Pharm Bull. 2021;11:28–38.
17. Alghoraibi I, Alomari S. Different methods for nanofiber design and fabrication. In: Barhoum A, Bechelany M, Makhlouf A, editors. Handbook of nanofibers. Cham: Springer International Publishing; 2018. p. 1–46.
18. Abdelaziz D, Hefnawy A, Al-Wakeel E, El-Fallal A, El-Sherbiny IM. New biodegradable nanoparticles-in-nanofibers based membranes for guided periodontal tissue and bone regeneration with enhanced antibacterial activity. J Adv Res. 2021;28:51–62.
19. Xue J, He M, Niu Y, Liu H, Crawford A, Coates P, Chen D, Shi R, Zhang L. Preparation and in vivo efficient anti-infection property of GTR/GBR implant made by metronidazole loaded electrospun polycaprolactone nanofiber membrane. Int J Pharm. 2014;475:566–77.
20. Dos Santos DM, Chagas PAM, Leite IS, Inada NM, de Annunzio SR, Fontana CR, Campana-Filho SP, Correa DS. Core-sheath nanostructured chitosan-based nonwovens as a potential drug delivery system for periodontitis treatment. Int J Biol Macromol. 2020;142:521–34.
21. Xu C, Lei C, Meng L, Wang C, Song Y. Chitosan as a barrier membrane material in periodontal tissue regeneration. J Biomed Mater Res B Appl Biomater. 2012;100:1435–43.
22. Goy, R.C.; Britto, D.d. and Assis, O.B.G., A review of the antimicrobial activity of chitosan. *Polímeros* 2009, *19*.
23. Qasim SSB, Nogueria LP, Fawzy AS, Daood U. The effect of cross-linking efficiency of drug-loaded novel freeze gelated chitosan templates for periodontal tissue regeneration. AAPS PharmSciTech. 2020;21:173.
24. Kanwal A, Iqbal A, Arshad R, Akhtar S, Razzaq S, Ahmad NM, Naz H, Shahnaz G. Formulation and evaluation of novel thiolated intra pocket periodontal composite membrane of doxycycline. AAPS PharmSciTech. 2019;20:325.
25. Tawfik EA, Alshamsan A, Abul Kalam M, Raish M, Alkholief M, Stapleton P, Harvey K, Craig DQM, Barker SA. In vitro and in vivo biological assessment of dual drug-loaded coaxial nanofibers for the treatment of corneal abrasion. Int J Pharm. 2021;604:120732.
26. Cho YD, Kim KH, Lee YM, Ku Y, Seol YJ. Periodontal wound healing and tissue regeneration: a narrative review. Pharmaceuticals (Basel). 2021;14(5):456.
27. Yoshimoto I, Sasaki JI, Tsuboi R, Yamaguchi S, Kitagawa H, Imazato S. Development of layered PLGA membranes for periodontal tissue regeneration. Dent Mater. 2018;34:538–50.
28. Zhao S, Pinholt EM, Madsen JE, Donath K. Histological evaluation of different biodegradable and non-biodegradable membranes

implanted subcutaneously in rats. J Craniomaxillofac Surg. 2000;28:116–22.
29. Ranch KM, Maulvi FA, Koli AR, Desai DT, Parikh RK, Shah DO. Tailored doxycycline hyclate loaded in situ gel for the treatment of periodontitis: optimization, *in vitro* characterization, and antimicrobial studies. AAPS PharmSciTech. 2021;22:77.
30. Triplett RG, Schow SR. Autologous bone grafts and endosseous implants: complementary techniques. J Oral Maxillofac Surg. 1996;54:486–94.
31. Abou Neel EA, Bozec L, Knowles JC, Syed O, Mudera V, Day R, Hyun JK. Collagen — emerging collagen based therapies hit the patient. Adv Drug Deliv Rev. 2013;65:429–456.
32. Zupancic S, Kocbek P, Baumgartner S, Kristl J. Contribution of nanotechnology to improved treatment of periodontal disease. Curr Pharm Des. 2015;21:3257–71.
33. Darby I. Periodontal materials. Aust Dent J. 2011;56:107–18.
34. Xu L, Li W, Sadeghi-Soureh S, Amirsaadat S, Pourpirali R, Alijani S. Dual drug release mechanisms through mesoporous silica nanoparticle/electrospun nanofiber for enhanced anticancer efficiency of curcumin. J Biomed Mater Res A. 2022;110:316–30.
35. Lan X, Liu Y, Wang Y, Tian F, Miao X, Wang H, Tang Y. Coaxial electrospun PVA/PCL nanofibers with dual release of tea polyphenols and ε-poly (L-lysine) as antioxidant and antibacterial wound dressing materials. Int J Pharm. 2021;601: 120525.
36. Xue J, He M, Liang Y, Crawford A, Coates P, Chen D, Shi R, Zhang L. Fabrication and evaluation of electrospun PCL–gelatin micro-/nanofiber membranes for anti-infective GTR implants. J Mater Chem B. 2014;2:6867–77.
37. Abdel Hady M, Sayed OM, Akl MA. Brain uptake and accumulation of new levofloxacin-doxycycline combination through the use of solid lipid nanoparticles: formulation; optimization and in-vivo evaluation. Colloids Surf B Biointerfaces. 2020;193: 111076.
38. Mehrandish S, Mohammadi G, Mirzaeei S. Preparation and functional evaluation of electrospun polymeric nanofibers as a new system for sustained topical ocular delivery of itraconazole. Pharm Dev Technol. 2022;27:25–39.
39. Taghe S, Mirzaeei S. Preparation and characterization of novel, mucoadhesive ofloxacin nanoparticles for ocular drug delivery. Braz J Pharm Sci. 2019;55:1–12.
40. Çay A, Miraftab M, Perrin Akçakoca Kumbasar E. Characterization and swelling performance of physically stabilized electrospun poly(vinyl alcohol)/chitosan nanofibres. Eur Polym J. 2014;61:253–262.
41. Wen P, Zong M-H, Linhardt RJ, Feng K, Wu H. Electrospinning: a novel nano-encapsulation approach for bioactive compounds. Trends Food Sci Technol. 2017;70:56–68.
42. Gagandeep Garg T, Malik B, Rath G, Goyal AK. Development and characterization of nano-fiber patch for the treatment of glaucoma. Eur J Pharm Sci. 2014;53:10–6.
43. Taghe S, Mirzaeei S, Ahmadi A. Preparation and evaluation of nanofibrous and film-structured ciprofloxacin hydrochloride inserts for sustained ocular delivery: pharmacokinetic study in rabbit's eye. Life. 2023;13(4):913.
44. Choo K, Ching YC, Chuah CH, Julai S, Liou NS. Preparation and characterization of polyvinyl alcohol-chitosan composite films reinforced with cellulose nanofiber. Materials (Basel). 2016;9(8):644.
45. Raz P, Brosh T, Ronen G, Tal H. Tensile properties of three selected collagen membranes. Biomed Res Int. 2019;2019:5163603.
46. Ngadiman NHA, Mohd Yusof N, Idris A, Shakir A, Kurniawan D. Influence of polyvinyl alcohol molecular weight on the electrospun nanofiber mechanical properties. Procedia Manuf. 2015;2:568–572.
47. Chakrapani VY, Gnanamani A, Giridev VR, Madhusoothanan M, Sekaran G. Electrospinning of type I collagen and PCL nanofibers using acetic acid. J Appl Polym Sci. 2012;125:3221–7.
48. Arancibia R, Maturana C, Silva D, Tobar N, Tapia C, Salazar JC, Martínez J, Smith PC. Effects of chitosan particles in periodontal pathogens and gingival fibroblasts. J Dent Res. 2013;92:740–5.
49. Ikinci G, Senel S, Akincibay H, Kaş S, Erciş S, Wilson CG, Hincal AA. Effect of chitosan on a periodontal pathogen Porphyromonas gingivalis. Int J Pharm. 2002;235:121–7.
50. Wroblewska K, Kucinska M, Murias M, Lulek J. Characterization of new eye drops with choline salicylate and assessment of their irritancy by *in vitro* short time exposure tests. Saudi Pharm J. 2015;23:407–12.
51. Germershaus O, Mao S, Sitterberg J, Bakowsky U, Kissel T. Gene delivery using chitosan, trimethyl chitosan or polyethylenglycol-graft-trimethyl chitosan block copolymers: establishment of structure-activity relationships *in vitro*. J Control Release. 2008;125:145–54.
52. Alavarse AC, de Oliveira Silva FW, Colque JT, da Silva VM, Prieto T, Venancio EC, Bonvent J-J. Tetracycline hydrochloride-loaded electrospun nanofibers mats based on PVA and chitosan for wound dressing. Mater Sci Eng C. 2017;77:271–81.
53. Jia L-N, Zhang X, Xu H-Y, Hua F, Hu X-G, Xie Q, Wang W, Jia J. Development of a doxycycline hydrochloride-loaded electrospun nanofibrous membrane for GTR/GBR applications. J Nanomater. 2016;2016:6507459.
54. Norowski PA, Babu J, Adatrow PC, Garcia-Godoy F, Haggard WO, Bumgardner JD. Antimicrobial activity of minocycline loaded genipin-crosslinked nano-fibrous chitosan mats for guided tissue regeneration. J Biomater Nanobiotechnol. 2012;3(4):528.
55. Li W, Ding Y, Yu S, Yao Q, Boccaccini AR. Multifunctional chitosan-45S5 bioactive glass-poly(3-hydroxybutyrate-co-3-hydroxyvalerate) microsphere composite membranes for guided tissue/bone regeneration. ACS Appl Mater Interfaces. 2015;7:20845–54.
56. Mirzaeei S, Mansurian M, Asare-Addo K, Nokhodchi A. Metronidazole- and amoxicillin-loaded PLGA and PCL nanofibers as potential drug delivery systems for the treatment of periodontitis: in vitro and in vivo evaluations. Biomedicines. 2021;9(8):975.
57. Xue J, He M, Niu Y, Liu H, Crawford A, Coates P, Chen D, Shi R, Zhang L. Preparation and in vivo efficient anti-infection property of GTR/GBR implant made by metronidazole loaded electrospun polycaprolactone nanofiber membrane. Int J Pharm. 2014;475:566–77.
58. Tort S, Acartürk F, Beşikci A. Evaluation of three-layered doxycycline-collagen loaded nanofiber wound dressing. Int J Pharm. 2017;529:642–53.